Deep Chemometrics for Nondestructive-INPA 2020

by Kestrilia .

Submission date: 10-Mar-2020 10:40PM (UTC+0800)
Submission ID: 1272987153
File name: Kestrilia_Deep_Chemometrics_for_Nondestructive-INPA_2020.pdf (1.14M)
Word count: 6607
Character count: 35447

Available at www.sciencedirect.com

INFORMATION PROCESSING IN AGRICULTURE xxx (xxxx) xxx

journal homepage: www.elsevier.com/locate/inpa

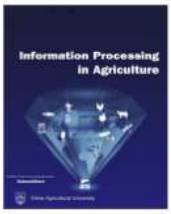

Deep chemometrics for nondestructive photosynthetic pigments prediction using leaf reflectance spectra

Kestrilia Rega Prilianti [a,*], Edi Setiyono [b], Oesman Hendra Kelana [a], Tatas Hardo Panintingjati Brotosudarmo [b]

[a] Department of Informatics Engineering, Universitas Ma Chung, Villa Puncak Tidar N-01, Malang 65151, Indonesia
[b] Ma Chung Research Center for Photosynthetic Pigments, Villa Puncak Tidar N-01, Malang 65151, Indonesia

ARTICLE INFO

Article history:
Received 27 May 2019
Received in revised form
20 November 2019
Accepted 8 February 2020
Available online xxxx

Keywords:
Convolutional neural network
Deep chemometrics
Leaf reflectance
Nondestructive method
Photosynthetic pigments

ABSTRACT

The need for the rapid assessment of the photosynthetic pigment contents in plants has encouraged the development of studies to produce nondestructive quantification methods. This need is driven by the fact that data on the photosynthetic pigment contents can provide a variety of important information that is related to plant conditions. Using deep chemometrics, we developed a novel one-dimensional convolutional neural network (CNN) model to predict the photosynthetic pigment contents in a nondestructive and real-time manner. Intact leaf reflectance spectra from spectroscopic measurements were used as the inputs. The prediction was simultaneously carried out for three main photosynthetic pigments, i.e., chlorophyll, carotenoid and anthocyanin. The experimental results show that the prediction accuracy is very satisfying, with a mean absolute error (MAE) = 0.0122 ± 0.0004 for training and 0.0321 ± 0.0022 for validation (data range of 0–1).

1. Introduction

Changes in photosynthetic pigment contents, especially chlorophylls, carotenoids and anthocyanins, are an important indicator to evaluate plant conditions. The composition is strongly influenced by the amount of light, oxygen, nutrients, water, and temperature of the environment in which the plant grows [1]. In addition to that, it can also be used as an indication of pest and disease attacks [2]. Therefore, a rapid method for determining the photosynthetic pigment contents is very essential in agricultural studies. With the rapid development of sensor and computer technology, the development of nondestructive methods for quantifying the photosynthetic pigment contents in plants has now become a popular topic [3].

The nondestructive methods for analyzing plants generally utilize the optical properties of the leaves. Feret et al. [4] developed PROSPECT-D which is the latest development of the PROSPECT models. PROSPECT was first conceived by Jacquemoud [5] which then also has developed into PROSPECT-4 and PROSPECT-5 [6]. PROSPECT is a radiative transfer model that represents three leaf optical properties, i.e., structure, pigment concentration (chlorophyll), and water content. In the PROSPECT-D model, several other properties are added

* Corresponding author at: Department of Informatics Engineering, Universitas Ma Chung, Villa Puncak Tidar N-01, Malang-East Java 65151, Indonesia.
E-mail address: kestrilia.rega@machung.ac.id (K.R. Prilianti).
Peer review under responsibility of China Agricultural University.
https://doi.org/10.1016/j.inpa.2020.02.001

Please cite this article as: K. R. Prilianti, E. Setiyono, O. H. Kelana et al., Deep chemometrics for nondestructive photosynthetic pigments prediction using leaf reflectance spectra, Information Processing in Agriculture, https://doi.org/10.1016/j.inpa.2020.02.001

especially to the pigment concentration. PROSPECT-D can represent the content of three main photosynthetic pigments simultaneously, i.e., chlorophyll, carotenoid and anthocyanin. PROSPECT models are used to simulate the directional–hemi spherical reflectance of various plant species over the solar spectrum from 400 nm to 2500 nm. The PROSPECT models were developed using mathematical formulations and claimed to be able to simulate realistic leaf optical properties with minimal error. Asner et al. [7,8] implement several statistical methods, i.e., ANOVA, hierarchical cluster, probabilistic diversity model and partial least square regression (PLSR) for the chemometric analysis to characterize the spectral properties of tropical forests in Australia. They found a linkage between the remotely sensed properties and the taxonomic of tropical forest canopies.

Gitelson et al. [9–12] developed several nondestructive methods for measuring the photosynthetic pigment contents using reflectance spectroscopy. They observed the relationship of the spectral behavior of leaf reflectance with the photosynthetic pigment contents. Mathematical formulations were then made based on the reflectance values at certain spectral bands. The chlorophyll content is known to be strongly correlated with the leaf reflectance at 550 ± 20 nm, 715 ± 20 nm, and 450 ± 20 nm and the Near Infrared (NIR) above 750 nm. The carotenoid content is known to be strongly correlated with the leaf reflectance at 510 ± 5 nm, 550 ± 15 nm and above 700 ± 7.5 nm. The anthocyanin content is known to be strongly correlated with the leaf reflectance at 550 ± 15 nm and 705 ± 5 nm [9]. However, due to the diversity of plant responses to the environment, the reflectance behavior of the photosynthetic pigments can easily shift from what has been formulated by Gitelson to other different adjacent spectral range [13]. Moreover, it is known that the relationships between the reflectance in the visible range and pigment contents are essentially nonlinear. Hence, the mathematical formulation to calculate the pigment contents can be very difficult and can easily be inaccurate.

In this study, we applied deep chemometrics, which is the implementation of deep learning concepts in chemometrics. We proposed the use of a convolutional neural network (CNN) method that can process the entire leaf reflectance spectrum and, more importantly, it can show nonlinear relationships very well without complicated mathematical models and formulations. Using this artificial intelligence-based method, we can train the system to be able to study the variations in the reflectance shifts at other adjacent spectral range. The CNN can produce simultaneous predictions of the three photosynthetic pigment contents, i.e., chlorophyll, carotenoid and anthocyanin. Generally, the CNN is used to process digital image data that have at least two dimensions. In our previous study, we have evaluated the application of CNN to process plant leaves digital images to predict its photosynthetic pigments, i.e., chlorophyll, carotenoid and anthocyanin [14]. The results show that CNN's performance is superior in representing nonlinear models that connect plant digital images with its photosynthetic pigment contents. In this work, we evaluated the performance of CNN to predict photosynthetic pigment contents in plant leaves using its reflectance spectrum measured by a spectrometer. Since the leaf reflectance spectrum is of one dimension, we used a variant of the CNN known as the one-dimensional CNN (1D-CNN). This 1D-CNN is popularly used in speech recognition [15] and time series analysis [16]. However, Malek et al. [17] has claimed that 1D-CNN has also an outstanding ability in spectroscopic signal regression. Liu et al. [18] applied the 1D-CNN to process Raman spectroscopic data and it is known that the 1D-CNN can well recognize Raman spectra from the RRUFF database for mineral classifications. Ng et al. [19] explored the used of 1D-CNN for simultaneous prediction of several soil properties and found that two-channel 1D-CNN model was the best compared to Cubist tree and PLSR models. Therefore, we believed that the 1D-CNN can also be used to process reflectance spectroscopic data. We hypothesized that this method can well recognize the leaf reflectance spectrum to distinguish the types of pigments that are represented by it. Moreover, unlike most applications of the CNN, our 1D-CNN architecture was designed to produce predictions rather than classifications. We also introduced a way to train 1D-CNNs with small amounts of data that still provide good accuracy.

2. Material and methods

2.1. Sample preparation

The samples were taken from four Indonesian herbal plant species, i.e., *Syzigium oleana*, *Piper betle*, *Jasminum* and *Graptophyllum pictum*. The diversity of age, color, and position from the terminal bud were also considered when preparing the samples. Each individual leaf were taken while ensuring the availability of complete colors variations from each plant species. We also ensure the availability of variations in pigments content by taking leaves from various positions from the terminal bud. Leaves that are close to the terminal bud are generally younger than leaves that are further from the terminal bud. In addition, we found that the lower leaves (afar from the terminal bud) were less exposed to sunlight than the upper leaves (near the terminal bud). Those factors naturally create diversity in the leaves pigment contents. A total of 212 individual fresh leaves were taken from August to November 2018 from several regions in Malang, East Java, Indonesia. Those species with its diversity in some traits were carefully selected concerning the CNN's need to learn variations in the input spectrum. Taking into account that the model will predict three types of photosynthetic pigments, i.e. chlorophyll, carotenoid and anthocyanin, the variation of those pigments content should be well provided. *Jasminum* was used to represent the data related to variations in the chlorophyll and carotenoid content, *S. oleana* was used for the carotenoid and anthocyanin content and *G. pictum* was used for the anthocyanin content. If these three varieties are dominated by certain pigment contents, this is not the case with *P. betle*. Therefore, *P. betle* was used to complement the other variations that cannot be measured from the other three varieties. Fig. 1 depicts the examples of the leaves that were used in the experiment. We consider the characteristics of the four spe-

Please cite this article as: K. R. Prilianti, E. Setiyono, O. H. Kelana et al., Deep chemometrics for nondestructive photosynthetic pigments prediction using leaf reflectance spectra, Information Processing in Agriculture, https://doi.org/10.1016/j.inpa.2020.02.001

Fig. 1 – The example of the leaves that were used in the experiment: (a) *Jasminum*, (b) *S. oleana*, (c) *G. pictum*, and (d) *P. betle*.

cies are sufficient enough to meet the initial learning needs of the CNN. The hyperparameter generated from the training process can later be used as a good parameter initialization for the future training with additional data from new species.

2.2. Data acquisition

Each sample underwent two data acquisition processes in the same day, the dry lab-based and the wet lab-based. The dry lab-based data acquisition measures the leaf reflectance using a USB-4000 reflectance spectrometer (Ocean Optics, Inc., Dunedin, Forida, USA) with optical resolution 0.1–10 nm. Tungsten halogen (Ocean Optics HL-2000 family) with wavelength range 360–2400 nm was used as the light resource. The results included 212 spectra, which were measured over a spectral range from 345 nm up to 1041 nm with 0.22 nm step. We used barium sulfate (BaSO4) as a standard to measure the reflectance of each leaf. Fig. 2 depicts an example of the spectra. It can be seen that the difference in the amount of chlorophyll, carotenoid and anthocyanin along with its composition tend to produces different reflectance patterns. Moreover, water content, differences in leaf structure, thickness, and surface reflection can also make spectrum patterns vary widely. These factors are the other source of the main difficulties of pigment contents prediction in plant leaves using its reflectance spectrum. However, Gitelson and Merzlyak [9] have shown that adjustments to the calculation of pigment content influenced by these factors can be done by analyzing reflectance in the NIR and blue ranges. Thus, a thorough analysis of reflectance at various wavelengths should be able to improve the accuracy of the prediction of pigment contents.

The wet lab-based data acquisition calculated the pigment content using a method that was proposed by Lichtentaler

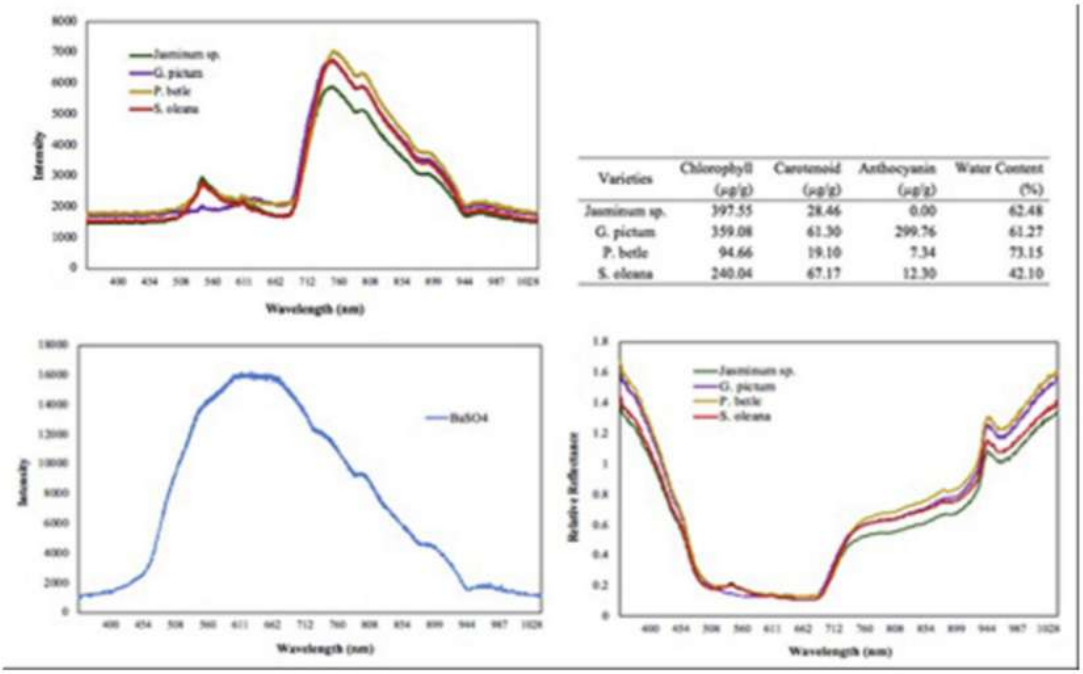

Varieties	Chlorophyll (μg/g)	Carotenoid (μg/g)	Anthocyanin (μg/g)	Water Content (%)
Jasminum sp.	397.55	28.46	0.00	62.48
G. pictum	359.08	61.30	299.76	61.27
P. betle	94.66	19.10	7.34	73.15
S. oleana	240.04	67.17	12.30	42.10

Fig. 2 – The spectra that were measured from four different varieties of leaves with their corresponding photosynthetic pigment contents. The $BaSO_4$ standard was used to measure the relative reflectance.

Please cite this article as: K. R. Prilianti, E. Setiyono, O. H. Kelana et al., Deep chemometrics for nondestructive photosynthetic pigments prediction using leaf reflectance spectra, Information Processing in Agriculture, https://doi.org/10.1016/j.inpa.2020.02.001

[20] for chlorophyll and carotenoid and a method that was proposed by Sims and Gammon [21] for anthocyanin. Each leaf was divided into two equal sized parts. The first part was utilized for the chlorophyll and carotenoid quantifications. The second part was utilized for the anthocyanin quantification. Each part was crushed into small pieces with a mortar and pestle, and up to 0.05 g were taken and put into different tubes. The CaCO3 and sodium ascorbate powder with 1.5 mL of solvent (100% acetone for chlorophyll and carotenoid; and a mixture of methanol, concentrated hydrochloric acid and distilled water for anthocyanin) was then added into the tubes to extract the pigments. The tubes were then rotated using a vortex for 1 min to homogenize the mixtures and then cooled using ice for another 1 min. After repeating this process three times with the vortex, all tubes were centrifuged for two minutes at a speed of 14,000 rpm and cooled again with ice. The last step was the absorbance measurement using a UV-1800 double-beam UV/VIS scanning spectrophotometer (Shimadzu Corp., Kyoto, Japan). The absorbance values were then converted into pigment contents. Finally, for each individual leaf sample, three data were obtained, i.e., the chlorophyll content, the carotenoid content and the anthocyanin content.

2.3. Dataset preparation

Each spectrum (in the form of a csv file) was paired with the pigment content data. The pigment contents were normalized into a 0–1 range using Eq. (1), where z is the normalized data and x is the raw data:

$$z = \frac{x - \min(x)}{[\max(x) - \min(x)]} \tag{1}$$

This process is important considering that the natural amount of each pigment content is quite different. Chlorophyll content is in the range of hundreds to thousands, while carotenoid and anthocyanin are only in the range of tens. Thus, the normalization will ensure that each neuron (filters) in the CNN model has an equal opportunity to learn the pattern of each pigment. Especially at the backpropagation step, when an error is propagated back to update the neuron weight. Therefore, there were 212 pairs of data, which were then made into two datasets, i.e., a training set (80%) and a validation set (20%). To ensure that the need for variation in the training set was met, the two data sets were randomly constructed prior to the training process.

2.4. Design of the 1D-CNN architecture

The input of the architecture was the intact leaf reflectance spectrum, and the output was the pigment content predictions, i.e., chlorophyll, carotenoid and anthocyanin. Fig. 3 depicts an example of a simple 1D-CNN architecture consisting of one convolution layer, one maximum pooling layer and one fully connected layer. The convolution was done using Eq. (2) [18], where $y^{(j)}$ is the output map, $x^{(i)}$ is the input map, $b^{(j)}$ is the bias parameter and $k^{(ij)}$ is the convolution kernel between maps i and j:

$$y^{(j)} = f\left(b^{(j)} + \sum_i k^{(ij)} * x^{(i)}\right) \tag{2}$$

The ReLu activation function was used in the convolution layer. Eq. (3) shows the ReLu formula, where $h^{(i)}$ is the hidden unit activation and x is the input:

$$h^{(i)} = \begin{cases} 0, & x < 0 \\ x, & x \geq 0 \end{cases} \tag{3}$$

Meanwhile, the LeakyReLu [22] activation function was used in the output nodes to avoid a dead ReLu. Eq. (4) shows the formula, where $w^{(i)}$ is the weight vector for the i^{th} hidden unit and x is the input:

$$h^{(i)} = \max\left(w^{(i)T}x, 0\right) = \begin{cases} w^{(i)T}x, & w^{(i)T}x > 0 \\ 0.1w^{(i)T}x, & else \end{cases} \tag{4}$$

We evaluated six 1D-CNN architectures (Table 3): four of them are our original architectures (PNet), and the remaining two are the modified AlexNet [23] and VGGNet [24]. AlexNet

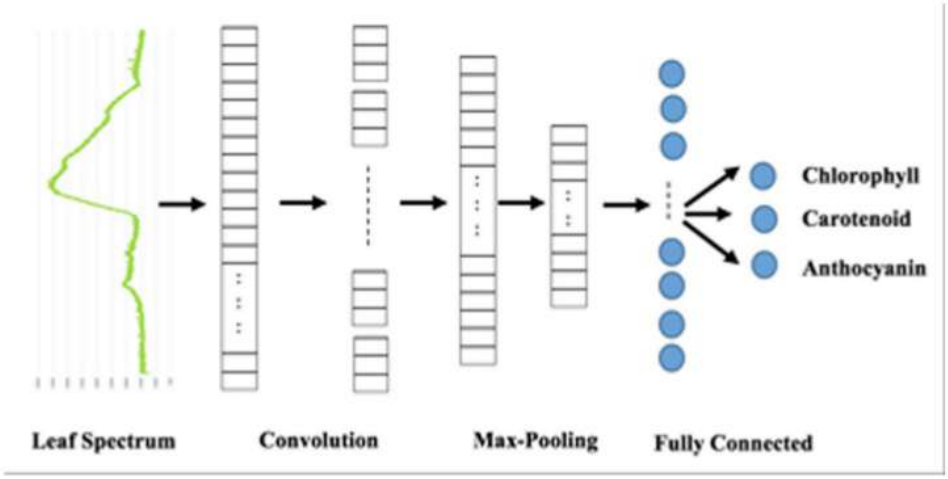

Fig. 3 – The example of the simple 1D-CNN architecture for photosynthetic pigment prediction.

Please cite this article as: K. R. Prilianti, E. Setiyono, O. H. Kelana et al., Deep chemometrics for nondestructive photosynthetic pigments prediction using leaf reflectance spectra, Information Processing in Agriculture, https://doi.org/10.1016/j.inpa.2020.02.001

Table 1 – The CNN architectures that are used in the experiment.

Layer		PNet_V1	PNet_V2	PNet_V3	PNet_V4	AlexNet	VGG-9
Input		1 × 3648	1 × 3648	1 × 3648	1 × 3648	1 × 3648	1 × 3648
Convolution	1	64 kernels in size 1 × 10 with max pooling	64 kernels in size 1 × 10 with max pooling	64 kernels in size 1 × 10 with max pooling	64 kernels in size 1 × 10 with max pooling	96 kernels in size 1 × 11 with max pooling	64 kernels in size 1 × 5
	2	–	64 kernels in size 1 × 5 with max pooling	64 kernels in size 1 × 5 with max pooling	64 kernels in size 1 × 5 with max pooling	256 kernels in size 1 × 5 with max pooling	64 kernels in size 1 × 3 with max pooling
	3	–	–	64 kernels in size 1 × 3 with max pooling	64 kernels in size 1 × 3 with max pooling	384 kernels in size 1 × 3 with max pooling	128 kernels in size 1 × 3
	4	–	–	–	64 kernels in size 1 × 3 with max pooling	384 kernels in size 1 × 3	128 kernels in size 1 × 3 with max pooling
	5	–	–	–	–	256 kernels in size 1 × 3	256 kernels in size 1 × 3
	6	–	–	–	–	–	256 kernels in size 1 × 3
	7	–	–	–	–	–	256 kernels in size 1 × 3 with max pooling
Fully connected	1	300 nodes, ReLu	300 nodes, ReLu	300 nodes, ReLu	300 nodes, ReLu	4096 nodes, ReLu	4096 nodes, ReLu
	2	–	–	–	–	4096 nodes, ReLu	4096 nodes, ReLu
Output		3 nodes, LeakyReLu	3 nodes, LeakyReLu	3 nodes, LeakyReLu	3 nodes, LeakyReLu	3 nodes, LeakyReLu	3 nodes, LeakyReLu

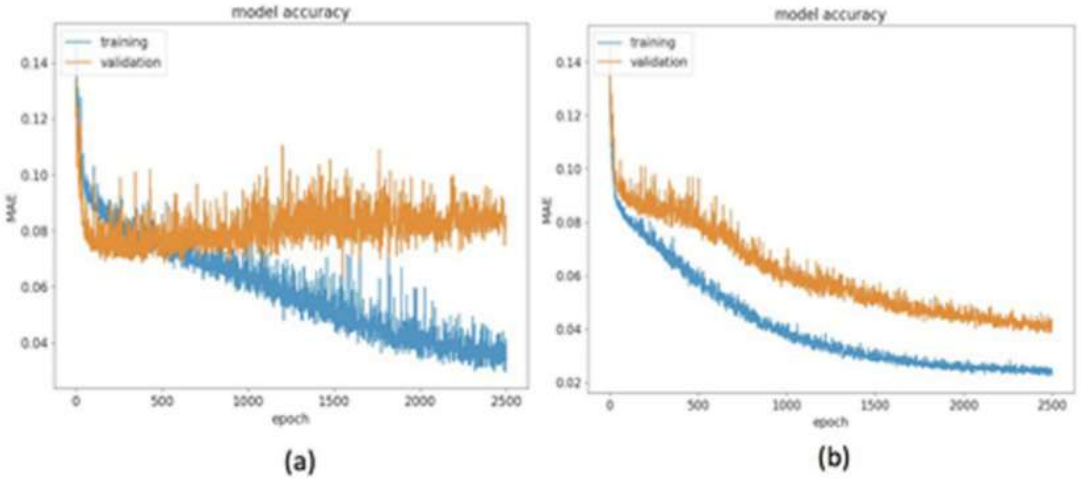

Fig. 4 – The MAE comparison of the application of data augmentation: (a) Without data augmentation, and (b) With data augmentation.

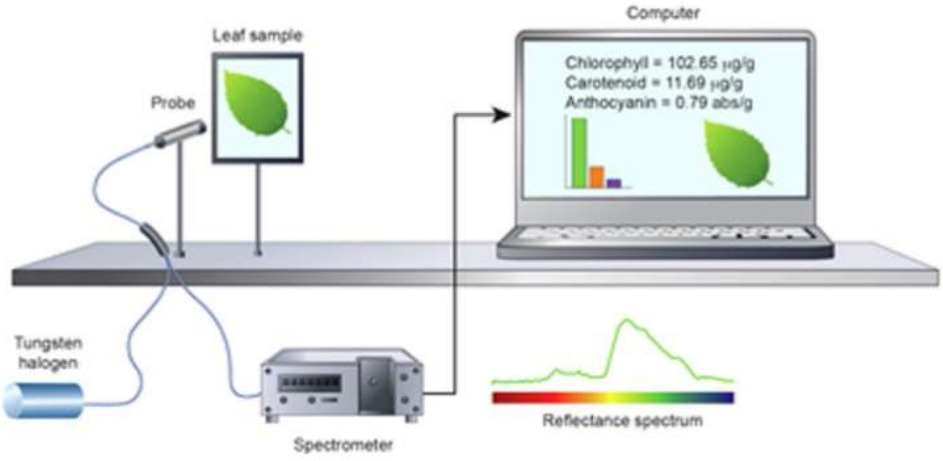

Fig. 5 – The device arrangement in the experiment.

and VGGNet were originally designed to receive multidimensional inputs. In this study, we modified them to be able to receive one-dimensional inputs. Likewise, the convolution layers were originally designed for two-dimensional convolutions, and we modified them for one-dimensional convolutions. Meanwhile, for the output layer, which was originally designed to represent the classes, we now used it to represent the chlorophyll, carotenoid and anthocyanin contents. Especially for the VGGNet, we also reduced the number of hidden layers (from the original sixteen down to nine). This is related to the issue of overfitting. With the small amount of training data, the number of 1D-CNN parameters that must be updated cannot be too large [25]. This issue will be discussed in the next subsection.

As seen in Table 1, the PNet_V1 is the simplest architecture, whereas the VGGNet-9 is the most complex architecture. The other architectures were designed with various levels of complexity between the PNet_V1 and VGGNet-9. Such designs were implemented to explore whether the increase of the architecture's complexity would be followed by the increase in its accuracy.

2.5. *Optimization methods*

Considering the ease of implementation, we trained our CNN architecture using gradient descent-based methods. This method is also known to be fast and efficient [26]. A total of seven gradient descent-based optimization methods were implemented and evaluated in this study, and then arranged the results from the simplest method to the latest modification. These methods included the Stochastic Gradient Descent (SGD) [26], Adaptive Gradient (Adagrad) [27], Adaptive Delta (Adadelta) [28], Root Mean Square Propagation (RMSProp) [29], Adaptive Momentum (Adam) [30], Adaptive

Please cite this article as: K. R. Prilianti, E. Setiyono, O. H. Kelana et al., Deep chemometrics for nondestructive photosynthetic pigments prediction using leaf reflectance spectra, Information Processing in Agriculture, https://doi.org/10.1016/j.inpa.2020.02.001

Max Pooling (Adamax) [30], and Nesterov Adaptive Momentum (Nadam) [31].

2.6. Performance indicator

In general, the CNN is applied to classification tasks. However, in this study, we applied the CNN to the regression task. Therefore, we used the mean absolute error (MAE) as the performance indicator. We also used it as the loss function during the backpropagation process. Eq. (5) is the formula of the MAE, where y_i is the actual pigment content, $\hat{y}_i$ is the predicted pigment content and n is the sample size. A good CNN architecture will result in a small MAE. Thus, the goal of the optimization methods is to minimize the MAE.

$$\mathrm{MAE} = \frac{1}{n}\sum_{i=1}^{n}|y_i - \hat{y}_i| \quad (5)$$

2.7. Data augmentation

The wet lab-based data acquisition involves laboratory procedures, which are time consuming and costly. Hence, in this study, we encountered the low sample size problem. Due to using only 212 spectra, all of the 1D-CNN architectures' training results show severe overfitting symptoms. Therefore, we applied a data augmentation technique to overcome the problem. Data augmentation is one of the recommended techniques to overcome overfitting. In addition, data augmentation is also proven to increase the robustness and training process of the CNN architecture [32]. Fig. 4 shows the example of MAE comparison without and with data augmentation. The CNN architecture is the PNet_V3, the optimization method is Nadam with 2500 epochs. It can be inferred that the implementation of data augmentation can significantly reduce overfitting issues. Thus, we applied random multiplications to the existing spectra to augment the dataset [33].

2.8. Experimental setup

Fig. 5 depicts the overall arrangement of the devices that were used in the experiment. The leaf samples were exposed to the light produced by the Tungsten halogen lamp. The leaf then produced a reflectance spectrum detected by the spectrometer. The spectrum then became the input for the 1D-CNN architecture to predict the chlorophyll, carotenoid and anthocyanin contents. The 1D-CNN architecture was developed using Python 2. The Keras API with the TensorFlow backend was also implemented to enable fast calculations. The CNN was run on a personal computer with an Intel Core i5 1.6 GHz processor, 8 GB of DDR3 RAM, and the macOS Sierra operating system. Prior to the prediction of the new data, the CNN architecture was trained using our existing dataset.

3. Result and discussions

3.1. Pigment content and composition

Table 2 shows the statistical summary of the wet lab-based data. It can be seen that *G. pictum* and *S. oleana* leaves contain more anthocyanin than the other three varieties, whereas *Jasminum* contains more chlorophyll and carotenoid. Since *P. betle* does not have a certain dominant pigment among all, it fills in the variations that do not exist. Moreover, it is important to ensure that all variations in the pigment content can be well represented by the existing leaf samples. The large standard deviation indicates that the pigment contents and composition in the leaves varied widely. Therefore, sufficient variations has been successfully provided in this study.

3.2. Model development and validation

Table 3 summarizes the experimental results of the six CNN architectures described in Section 2.4. For each architecture, ten training processes were carried out. We use Adamax

Table 2 – Statistical summary of the wet lab-based data.

Variety	∑ samples	Anthocyanin (μg/g)*		Carotenoid (μg/g)*		Chlorophyll (μg/g)*	
		Mean	St.Dev.	Mean	St.Dev.	Mean	St.Dev.
Syzigium oleana	62	59.45	73.33	31.97	32.84	124.21	147.95
Piper betle	44	4.58	6.61	8.94	9.92	30.48	37.23
Jasminum	55	0.00	0.00	44.24	39.29	306.57	171.83
Graptophyllum pictum	51	47.32	67.42	26.58	26.08	169.75	161.54

* Pigment content relative to the dry weight of the leaf material.

Table 3 – The MAE comparison of the six different CNN architectures.

Architecture	PNet_V1	PNet_V2	PNet_V3	PNet_V4	AlexNet	VGG-9
Training	0.0508 ± 0.0013	0.0411 ± 0.0012	**0.0122 ± 0.0004**	0.0277 ± 0.0009	0.2710 ± 0.0011	0.1334 ± 0.0017
Validation	0.0671 ± 0.0056	0.0855 ± 0.0033	**0.0321 ± 0.0022**	0.0451 ± 0.0030	0.2230 ± 0.0043	0.1399 ± 0.0041

Please cite this article as: K. R. Prilianti, E. Setiyono, O. H. Kelana et al., Deep chemometrics for nondestructive photosynthetic pigments prediction using leaf reflectance spectra, Information Processing in Agriculture, https://doi.org/10.1016/j.inpa.2020.02.001

optimization method for AlexNet, Adam for VGG-9 [34] and Nadam for PNet. The five smallest MAE values were then averaged and used as the performance indicator. Each training process was stopped after 2500 epochs. Above the 2500th epoch, the training and validation MAEs did not show significant changes and, in some architectures, the difference between the two values tended to increase. The PNet_V3 architecture had the best performance, while the AlexNet and VGG-9 were the worst. From this result, it can be concluded that a highly complex architecture is not suitable for the photosynthetic pigment prediction task. All our PNet architectures clearly outperformed the AlexNet and VGG-9. Among the PNet architectures, the simplest one (PNet_V1) provided the worst MAE. The addition of the convolution layer has been shown to decrease the MAE (see PNet_V2 and PNet_V3). However, to a certain extent, the further addition of more convolution layers resulted in larger MAEs (see PNet_V4). Hence, PNet_V3 with three convolution layers has been chosen as the best architecture.

Prilianti et al. [34] has shown that the training performance of the 3D-CNN architectures is also dependent on the selected optimization method as is also the case with the common development of deep learning-based models [35]. Therefore, we explored the performance of seven optimization methods with the PNet_V3, i.e., the SGD, Adagrad, Adadelta, RMSProp, Adam, Adamax and Nadam. We also applied the batch gradient descent to provide a more stable error gradient, which resulted in more stable convergence. The best batch size in our experiment was 135. Fig. 6 shows the result. It can be seen that the different optimization methods had significant impacts on the decrease in the MAE. The SGD optimization method appears to have had the worst performance. However, the SGD provided the smallest difference between its training and validation MAEs among all the methods. This result shows that training using the SGD can greatly reduce the risk of overfitting. Modification to the SGD could improve the results of the training process. In Fig. 6, the optimization methods are sorted from the oldest to the most recent (left to right), where the newer optimization method is actually a modification of the previous method. It appears that the MAE continues to decrease along with the modifications to the optimization method. The Nadam optimization method finally provided the best results among all.

In previous studies, Huang et al. [36] showed that the prediction of the chlorophyll content can be disrupted by the presence of anthocyanin. This causes higher errors in the prediction of chlorophyll content. Fig. 7 shows the comparison of the validation absolute error of the anthocyanin, carotenoid and chlorophyll predictions by the P3Net_V3 using Nadam

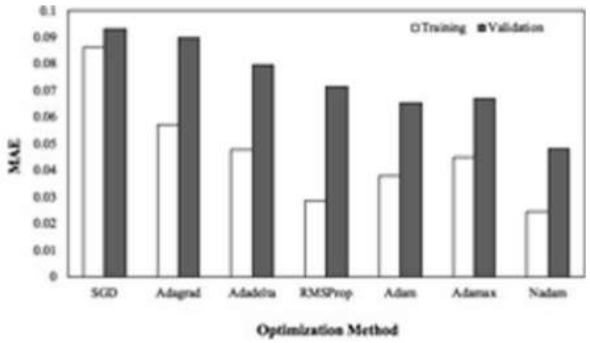

Fig. 6 – Performance comparison of the seven optimization methods with the PNet_V3.

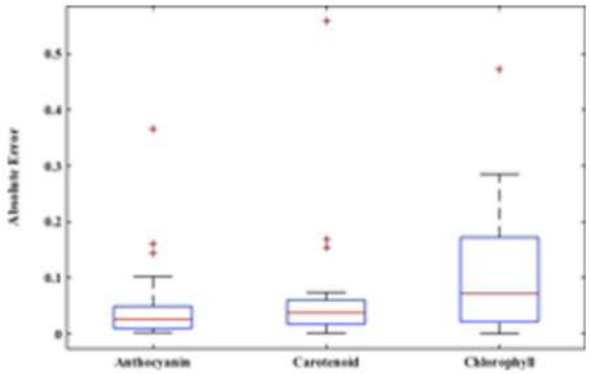

Fig. 7 – Comparison of the validation absolute error for each pigment.

Please cite this article as: K. R. Prilianti, E. Setiyono, O. H. Kelana et al., Deep chemometrics for nondestructive photosynthetic pigments prediction using leaf reflectance spectra, Information Processing in Agriculture, https://doi.org/10.1016/j.inpa.2020.02.001

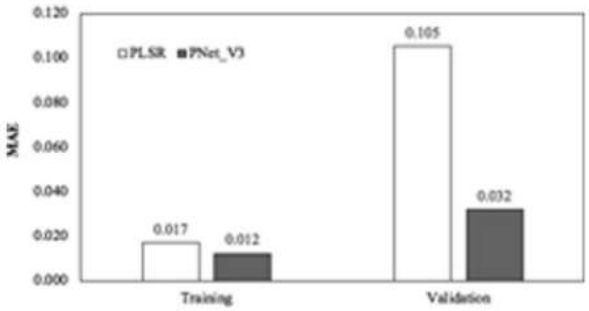

Fig. 8 – Performance comparison of PLSR and PNet_V3 on validation data.

optimization method. It depicts the distribution of absolute error values for each prediction of pigment content for each validation data. The same phenomenon also occurred in this study as that revealed by Huang et al. More than 50% of leaf samples that were used in our experiment contained anthocyanin. This tended to cause the training MAE of the chlorophyll prediction to be higher than that of the other two pigments. In addition to the higher average, the standard deviation was also larger. This indicates that the accuracy of the chlorophyll prediction was volatile. Moreover, as happened in the chlorophyll prediction, we also found that the MAE for the carotenoid predictions was also slightly higher than that of the anthocyanin predictions. Its standard deviation was also larger. This phenomenon has never been reported before. However, Gitelson et al. [6] stated that the carotenoid content has a very strong correlation with the chlorophyll content. Their experiment also showed that the anthocyanin, carotenoid and chlorophyll reflectances overlap in the green spectral range. Thus, the disruption of the reflectance measurement of chlorophyll due to the presence of anthocyanin also affects the carotenoid reflectance measurement. How to overcome this problem still cannot be determined in this study and will be a part of our future research.

3.3. *Comparison with previously developed models*

Partial Least Square Regression (PLSR) model is one of the widely implemented method in chemometrics [37]. Various spectroscopic techniques are being combined with PLSR as it can process large chemical data. We developed a PLSR model of our dataset and compared it with our 1D-CNN model. The model we built (PNet_V3) proved to be superior for the prediction of new data (validation data). The PLSR model is good in its accuracy for predicting training data but very poor in its accuracy for predicting validation data. Fig. 8 depict the performance comparison of PLSR and PNet_V3 on the validation data. The validation MAE of PLSR is much higher than the validation MAE of PNet_V3. It can be concluded that the generalization ability of the PNet_V3 model is far superior to PLSR. Moreover as is generally the case of regression analysis, PLSR is sensitive to outliers which will often be found in plant pigment analysis.

Compared to the PROSPECT model, our model offers ease of implementation, it does not require other parameters as input. The PROSPECT model requires users to inform leaf structures, brown pigments, dry matter and water thickness to simulate a spectrum. Without proper expertise the user will certainly have difficulty determining these data. Moreover, in the PROSPECT model, the distribution of water content and pigment is considered uniform. Our model can properly recognize data patterns with a high level of nonlinearity. In addition, our model can always undergo retraining with new data to improve the accuracy of its predictions. Therefore, with high learning ability, additional inputs are not required to accompany leaf spectrum data.

4. Conclusion and future work

In this research, we have succeeded in developing a novel nondestructive method to predict the contents of the three main photosynthetic pigments, i.e., chlorophyll, carotenoid and anthocyanin, in plant leaves. The method was developed using a deep chemometric method that has been on the rise recently, i.e., the convolutional neural network (CNN). In addition to easier input handling, the CNN also provides faster predictions, thereby allowing for real-time and in situ analyses. This method is very well known for its success in handling multidimensional data. However, in this research, a 1D-CNN model was applied for the spectrum data, which was the output of the leaf reflectance measurements from the spectroscopic method. We named our architecture PNet, develop several versions and compared them. We found that PNet_V3 to be the best among all. Our PNet_V3 architecture achieved accuracies (measured using the MAE) of 0.0122 ± 0.0004 for training and 0.0321 ± 0.0022 for validation (data range of 0–1). The overfitting problems due to low amounts of data were successfully handled by applying data augmentation. However, despite the success of the overall MAE performance, we also reported differences in the performance of the PNet_V3 for predicting each of the three types of pigments. Anthocyanin was the most predictable pigment since the MAE of anthocyanin was the smallest when compared with the MAEs of carotenoid and chlorophyll. However, how this phenomenon can be corrected is beyond the aim of this research and will be studied in our coming future work.

Declaration of Competing Interest

The authors declared that there is no conflict of interest.

Please cite this article as: K. R. Prilianti, E. Setiyono, O. H. Kelana et al., Deep chemometrics for nondestructive photosynthetic pigments prediction using leaf reflectance spectra, Information Processing in Agriculture, https://doi.org/10.1016/j.inpa.2020.02.001

Acknowledgements

This work was funded by the Ministry of Research, Technology, and Higher Education of the Republic of Indonesia under Penelitian Dasar Unggulan Perguruan Tinggi (PDUPT) Scheme, (Grant No. 058/SP2H/LT/MONO/L7/2019).

REFERENCES

[1] Strever AE. Non-destructive assessment of leaf composition as related to growth of the grapevine (Vitis vinifera L. cv. Shiraz). Ph.D. Thesis, Stellenbosch University, Western Cape, South Africa; 2012.
[2] Jabeen A, Kiran TV, Subrahmanyam D, Lakshmi DL, Bhagyanarayana G, Khrisnaveni D. Variations in chlorophyll and carotenoid contents in tungro infected rice plants. J Res Dev 2017;5(1):2311–3278.
[3] Croft H, Chen JM. Leaf pigment content. Canada: Elsevier; 2017.
[4] Féret J, Gitelson AA, Noble SD, Jacquemoud S. PROSPECT-D: towards modeling leaf optical properties through a complete lifecycle. Remote Sens Environ 2017;193:204–15.
[5] Jacquemoud S, Baret F. PROSPECT: a model of leaf optical properties spectra. Remote Sens 1990;34:75–91.
[6] Feret JB, Francois C, Asner GP, Gitelson AA, Martin RE, Bidel RPL, et al. PROSPECT-4 and 5: advances in the leaf optical properties model separating photosynthetic pigments. Remote Sens Environ 2008;112:3030–43.
[7] Asner GP, Martin RE, Ford AJ, Metcalfe DJ, Liddell MJ. Leaf chemical and spectral diversity in Australian tropical forests. Ecol Appl 2009;19(1):236–53.
[8] Asner GP, Martin RE, Knapp DE, Tupayachi R, Anderson C, Carranza L, et al. Spectroscopy of canopy chemicals in humid tropical forests. Remote Sens Environ 2011;115(12):3587–98.
[9] Gitelson AA, Merzlyak MN. Non-destructive assessment of chlorophyll, carotenoid and anthocyanin content in higher plant leaves: principles and algorithms. In: Stamatiadis S, Lynch JM, Schepers JS, editors. Remote sensing for agriculture and the environment. Greece: Ella; 2004. p. 78–94.
[10] Gitelson AA, Keydan GP, Merzlyak MN. Three-band model for noninvasive estimation of chlorophyll, carotenoids, and anthocyanin contents in higher plant leaves. Geophys Res Lett 2006;33(L11402):1–5.
[11] Gitelson AA. Non-destructive estimation of foliar pigment (chlorophylls, carotenoids and anthocyanins) contents: espousing a semi-analytical three-band model. In: Thenkabail PS, Lyon JG, Huete A, editors. Hyperspectral remote sensing of vegetation. Taylor and Francis; 2011. p. 141–65.
[12] Gitelson A, Solovchenko A. Generic algorithms for estimating foliar pigment content. Geophys Res Lett 2017;44(18):9293–8.
[13] Gara TW, Darvishzadeh R, Skidmore AK, Wang T. Impact of vertical canopy position on leaf spectral properties and traits across multiple species. Remote Sens 2018;10:346.
[14] Prilianti KR, Onggara IC, Adhiwibawa MAS, Brotosudarmo THP, Anam S, Suryanto A. Multispectral imaging and convolutional neural network for photosynthetic pigments prediction. In 15th International conference on electrical engineering, computer science and informatics. EECSI 2018; 2018. p. 749–54.
[15] Collobert R, Puhrsch C, Synnaeve G. Wav2Letter: an end-to-end convnet-based speech recognition system. arXivpreprints arXiv:1609.03193v2; 2016.
[16] Singh P. Time series forecasting on crime data in Amsterdam for a software company. Information Management School, Universidade Nova de Lisboa; 2018.
[17] Malek S, Melgani F, Bazi Y. One-dimensional convolutional neural networks for spectroscopic signal regression: feature extraction based on 1D-CNN is proposed and validated. J Chemometr 2018;32(5) e2977.
[18] Liu J, Osadchy M, Ashton L, Foster M, Solomon CJ, Gibson SJ. Deep convolutional neural networks for raman spectrum recognition: a unified solution. arXivpreprints arXiv:1708.09022v1; 2017.
[19] Ng W, Minasny B, Montazerolghaem M, Padarian J, Ferguson R, Bailey S, et al. Convolutional neural network for simultaneous prediction of several soil properties using visible/near-infrared, mid-infrared, and their combined spectra. Geoderma 2019;352:251–67.
[20] Lichtenthaler HK. Chlorophyll and carotenoids: pigments of photosynthetic biomembranes. Methods Enzymol 1987;148:350–82.
[21] Sims DA, Gamon JA. Relationships between leaf pigment content and spectral reflectance across a wide range of species, leaf structures and developmental stages. Remote Sens Environ 2002;8:337–54.
[22] Maas AL, Hannun AY, Ng AY. Rectifiers nonlinearities improve neural network acoustic models. In 30th international conference on machine learning, 2013. ICML; 2013. p. 3.
[23] Krizhevsky A, Sutskever I, Hinton GE. ImageNet classification with deep convolutional neural networks. Adv Neural Inf Process Syst 2012;25:1–9.
[24] Simonyan K, Zisserman A. Very deep convolutional networks for large-scale image recognition. arXiv preprint arXiv:1409.1556; 2015.
[25] Truong TD, Nguyen VT, Tran MT. Lightweight deep convolutional network for tiny object recognition. In 7th international conference on pattern recognition applications and methods, 2018. ICPRAM; 2018. p. 675–82.
[26] Toulis P, Horel T, Airoldi EM. Stable robbins-monro approximations through stochastic proximal updates. arXiv preprint arXiv:1510.00967v3; 2018.
[27] Duchi J, Hazan E, Singer Y. Adaptive subgradient methods for online learning and stochastic optimization. J Mach Learn Res 2011;12:2121–59.
[28] Zeiler MD. ADADELTA: an adaptive learning rate method. arXiv preprint arXiv:1212.5701; 2012.
[29] Hinton G, Srivastava N, Swersky K. Overview of mini batch gradient descent. Computer Science Department, University of Toronto; 2015.
[30] Kingma DP, Ba JL. Adam a method for stochastic optimization. International conference on learning representations. ICLR, 2015.
[31] Dozat T. Incorporating nesterov momentum into adam. In: International conference in learning representation. ICLR. p. 2013–6.
[32] Aquino NMR, Gutoski M, Hattori L, Lopes HS. The effect of data augmentation on the performance of convolutional neural networks. In: 12th Brazilian congress on computational intelligence, 2017. CBIC; 2017.
[33] Bjerrum EJ, Glahder M, Skov T. Data augmentation for convolutional neural network (CNN) based deep chemometrics. arXiv preprint arXiv:1710.01927v1; 2017.
[34] Prilianti KR, Brotosudarmo THP, Anam S, Suryanto A. Performance comparison of the convolutional neural network optimizer for photosynthetic pigments prediction on plant digital image. In Symposium on biomathematics, 2018. SYMOMATH; 2018.

Please cite this article as: K. R. Prilianti, E. Setiyono, O. H. Kelana et al., Deep chemometrics for nondestructive photosynthetic pigments prediction using leaf reflectance spectra, Information Processing in Agriculture, https://doi.org/10.1016/j.inpa.2020.02.001

[35] Ruder S. An overview of gradient descent optimization algorithms, ArXiv preprint arXiv:1609.04747v2; 2017.
[36] Huang W, Lin K, Hsu M, Huang M, Yang Z, Chao P, et al. Eliminating interference by anthocyanin in chlorophyll estimation of sweet potato (Ipomoea batatas L.) leaves. Bot. Stud. 2014;55(1):11.
[37] Pawar HA, Kamat SR. Chemometrics and its application in pharmaceutical field. J. Phy. Chem. Biol. 2014;4(6):169.

Please cite this article as: K. R. Prilianti, E. Setiyono, O. H. Kelana et al., Deep chemometrics for nondestructive photosynthetic pigments prediction using leaf reflectance spectra, Information Processing in Agriculture, https://doi.org/10.1016/j.inpa.2020.02.001

Deep Chemometrics for Nondestructive-INPA 2020

ORIGINALITY REPORT

13%	7%	11%	7%
SIMILARITY INDEX	INTERNET SOURCES	PUBLICATIONS	STUDENT PAPERS

PRIMARY SOURCES

1	Submitted to Deakin University Student Paper	2%
2	ro.ecu.edu.au Internet Source	2%
3	Submitted to Ondokuz Mayıs Universitesi Student Paper	1%
4	Biyun Sheng, Fu Xiao, Letian Sha, Lijuan Sun. "Deep Spatial-temporal Model based Cross-scene Action Recognition Using Commodity WiFi", IEEE Internet of Things Journal, 2020 Publication	1%
5	Shibghatullah Muhammady, Yudhi Kurniawan, Andrivo Rusydi, Yudi Darma. "Electronic and magnetic properties of new half-metallic ferromagnetic rutile Ti1—V Ni O2 (x = y = 6.25%): A first-principles study", Journal of Physics and Chemistry of Solids, 2019 Publication	<1%
6	Submitted to University of Sydney Student Paper	<1%

7	Fitria Rahmawati, Leny Yuliati, Imam S. Alaih, Fatmawati R. Putri. "Carbon rod of zinc-carbon primary battery waste as a substrate for CdS and TiO 2 photocatalyst layer for visible light driven photocatalytic hydrogen production", Journal of Environmental Chemical Engineering, 2017 Publication	<1%
8	Kestrilia R. Prilianti, Ivan C. Onggara, Marcelinus A.S. Adhiwibawa, Tatas H.P. Brotosudarmo, Syaiful Anam, Agus Suryanto. "Multispectral Imaging and Convolutional Neural Network for Photosynthetic Pigments Prediction", 2018 5th International Conference on Electrical Engineering, Computer Science and Informatics (EECSI), 2018 Publication	<1%
9	"Computer Vision", Springer Science and Business Media LLC, 2017 Publication	<1%
10	Adhiwibawa, Marcelinus Alfasisurya Setya, Yonathan Eric Setiawan, Yusuf Setiawan, Kestrilia Rega Prilianti, and Tatas Hardo Panintingjati Brotosudarmo. "Application of Simple Multispectral Image Sensor and Artificial Intelligence for Predicting of Drought Tolerant Variety of Soybean", Procedia Chemistry, 2015. Publication	<1%

11	Qiu, Chen, Croft, Li, Zhang, Zhang, Ju. "Retrieving Leaf Chlorophyll Content by Incorporating Variable Leaf Surface Reflectance in the PROSPECT Model", Remote Sensing, 2019 Publication	<1%
12	res.mdpi.com Internet Source	<1%
13	Wartini Ng, Budiman Minasny, Maryam Montazerolghaem, Jose Padarian, Richard Ferguson, Scarlett Bailey, Alex B. McBratney. "Convolutional neural network for simultaneous prediction of several soil properties using visible/near-infrared, mid-infrared, and their combined spectra", Geoderma, 2019 Publication	<1%
14	uclouvain.be Internet Source	<1%
15	bmcimmunol.biomedcentral.com Internet Source	<1%
16	B. DATT. "Visible/near infrared reflectance and chlorophyll content in Eucalyptus leaves", International Journal of Remote Sensing, 9/20/1999 Publication	<1%
	Babita Majhi, Diwakar Naidu. "Pan Evaporation	

17	Modeling in Different Agroclimatic Zones using Functional Link Artificial Neural Network", Information Processing in Agriculture, 2020 Publication	<1%
18	www.sdiarticle2.org Internet Source	<1%
19	bioone.org Internet Source	<1%
20	Wei Su, Mingzheng Zhang, Dahong Bian, Zhe Liu, Jianxi Huang, Wei Wang, Jiayu Wu, Hao Guo. "Phenotyping of Corn Plants Using Unmanned Aerial Vehicle (UAV) Images", Remote Sensing, 2019 Publication	<1%
21	"Intelligent Data Engineering and Automated Learning – IDEAL 2018", Springer Science and Business Media LLC, 2018 Publication	<1%
22	jutisi.maranatha.edu Internet Source	<1%
23	pirhua.udep.edu.pe Internet Source	<1%
24	J.-B. Féret, A.A. Gitelson, S.D. Noble, S. Jacquemoud. "PROSPECT-D: Towards modeling leaf optical properties through a complete lifecycle", Remote Sensing of	<1%

Environment, 2017
Publication

25	Submitted to Birkbeck College Student Paper	<1%
26	"Medical Image Computing and Computer Assisted Intervention – MICCAI 2019", Springer Science and Business Media LLC, 2019 Publication	<1%
27	Submitted to The University of Manchester Student Paper	<1%
28	www.calmit.unl.edu Internet Source	<1%
29	Ramiro T. Gonzalez del Cerro, M.S.P Subathra, Nallapaneni Manoj Kumar, Sebastian Verrastro, S. Thomas George. "Modelling the daily reference evapotranspiration in semi-arid region of South India: A case study comparing ANFIS and empirical models", Information Processing in Agriculture, 2020 Publication	<1%
30	Lecture Notes in Computer Science, 2015. Publication	<1%
31	Daniela de Carvalho Lopes, Lorena de Oliveira Moura, Antonio José Steidle Neto, Leila de Castro Louback Ferraz et al. "Spectral Indices for Non-destructive Determination of Lettuce	<1%

Pigments", Food Analytical Methods, 2017
Publication

32	Feni Andriani, Iffatul Mardhiyah. "Blighted Ovum detection using convolutional neural network", AIP Publishing, 2019 Publication	<1%
33	Submitted to The Scientific & Technological Research Council of Turkey (TUBITAK) Student Paper	<1%
34	Mirzaei, Verrelst, Marofi, Abbasi, Azadi. "Eco-Friendly Estimation of Heavy Metal Contents in Grapevine Foliage Using In-Field Hyperspectral Data and Multivariate Analysis", Remote Sensing, 2019 Publication	<1%
35	Julien Morel, Sylvain Jay, Jean-Baptiste Féret, Adel Bakache, Ryad Bendoula, Francoise Carreel, Nathalie Gorretta. "Exploring the potential of PROCOSINE and close-range hyperspectral imaging to study the effects of fungal diseases on leaf physiology", Scientific Reports, 2018 Publication	<1%
36	s3.amazonaws.com Internet Source	<1%
37	Leny Yuliati, Peggy Tiong, Hendrik O Lintang. "Response surface methodology to optimize the	<1%

performance of reduced graphene oxide-mesoporous carbon nitride photocatalysts", Materials Research Express, 2019
Publication

38	Wartini Ng, Budiman Minasny, Wanderson de Sousa Mendes, José A. M. Demattê. "Estimation of effective calibration sample size using visible near infrared spectroscopy: deep learning vs machine learning", Copernicus GmbH, 2019 Publication	<1%
39	Submitted to Casuarina Senior College Student Paper	<1%
40	Submitted to Tennessee State University Student Paper	<1%

Exclude quotes	Off	Exclude matches	Off
Exclude bibliography	On		

Deep Chemometrics for Nondestructive-INPA 2020

GRADEMARK REPORT

FINAL GRADE

/0

GENERAL COMMENTS

Instructor

PAGE 1

PAGE 2

PAGE 3

PAGE 4

PAGE 5

PAGE 6

PAGE 7

PAGE 8

PAGE 9

PAGE 10

PAGE 11